PB91-226118

ANALYSIS OF EARTHQUAKE INDUCED SLOPE FAILURES: PHASE I TECHNICAL REPORT

WEIDLINGER ASSOCIATES, INCORPORATED
NEW YORK, NY

JUL 88

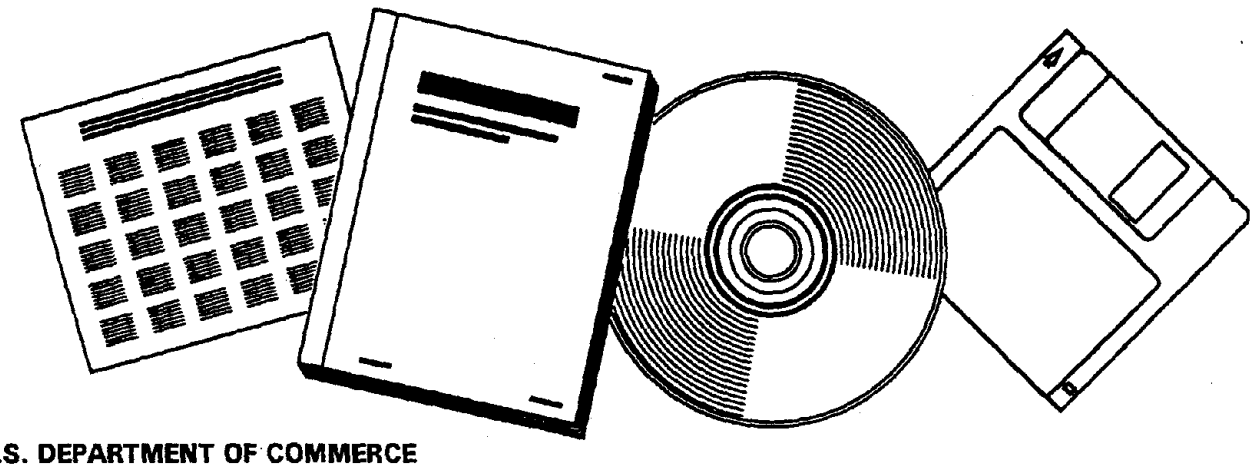

U.S. DEPARTMENT OF COMMERCE
National Technical Information Service

NSF/ISI-88150

PB91-226118

ANALYSIS OF EARTHQUAKE INDUCED SLOPE FAILURES

Ivan S. Sandler and Raymond P. Daddazio
Weidlinger Associates, Inc.
333 Seventh Avenue
New York, NY 10001

31 July 1988

Phase I Technical Report

THIS MATERIAL IS BASED UPON WORK SUPPORTED BY THE NATIONAL SCIENCE FOUNDATION UNDER AWARD NUMBER ISI-8760175. ANY OPINIONS,FINDINGS; AND CONCLUSIONS OR RECOMMENDATIONS EXPRESSED IN THIS PUBLICATION ARE THOSE OF THE AUTHOR(S) AND DO NOT NECESSARILY REFLECT THE VIEWS OF THE NATIONAL SCIENCE FOUNDATION.

50272-101

REPORT DOCUMENTATION PAGE	1. REPORT NO. NSF/ISI-88150	2.	3. PB91-226118

4. Title and Subtitle
Analysis of Earthquake Induced Slope Failures, Phase I Technical Report

5. Report Date
July 1988

6.

7. Author(s)
I.S. Sandler; R.P. Daddazio

8. Performing Organization Rept. No.

9. Performing Organization Name and Address
Weidlinger Associates
333 Seventh Avenue
New York, NY 10001

10. Project/Task/Work Unit No.

11. Contract(C) or Grant(G) No.
(C)
(G) ISI8760175

12. Sponsoring Organization Name and Address
Division of Industrial Science and Technological Innovation (ISTI)
Directorate for Scientific, Technological, and International Affairs (STIA)
National Science Foundation, Washington, DC 20550

13. Type of Report & Period Covered
SBIR Phase I

14.

15. Supplementary Notes

16. Abstract (Limit: 200 words)

Rational methods for seismic slope stability analysis require the prediction of critical state displacement behavior of an embankment. The use of advanced plasticity models, which satisfy the requirements of continuity and uniqueness of solution and have the capability of simulating a wide range of real effects in soils, is essential in this type of analysis. The focus of the research was the development of a simplified cap type plasticity model specialized for seismic analysis of embankments. The specific objectives that were met are: (1) the incorporation of a viscoelastic stress-strain relation into the cap model to simulate cyclic hysteresis below the yield surface, and (2) the incorporation of simplifying assumptions into the model in order to reduce the number of parameters necessary to fit the model to properties which can be obtained from data most typically available to geotechnical engineers.

17. Document Analysis a. Descriptors

Earthquakes
Landslides
Slopes
Plastic properties
Seismology
Embankments
Soils
Stability

b. Identifiers/Open-Ended Terms

c. COSATI Field/Group

18. Availability Statement	19. Security Class (This Report)	21. No. of Pages
NTIS	20. Security Class (This Page)	22. Price

Introduction

Slope failures, resulting from earthquakes, often cause extensive damage to lifeline systems and transportation networks. When they occur in highly populated regions, they may lead to loss of life. There is a need to develop more rational methods to assess the seismic stability of slopes.

Conventional methods used in evaluating seismic slope stability are usually described by the adjective pseudostatic (Newmark 1965, Seed 1966, Chen et al. 1978, and Chugh 1982, for example). In these methods, the inertia force, generated by the earthquake ground motion, is treated as an equivalent horizontal force, applied at the center of mass of a critical section of soil which has been defined by limit equilibrium methods. Although these methods have many shortcomings (Seed 1966, Seed and Martin 1966, Chen et al. 1978 and Chen 1980), they are simple to implement and are usually adequate. However, the use of these methods can sometimes be misleading, (Seed 1970).

A rational method for seismic slope stability analysis requires the simulation of progressive failure of a slope. The use of simple, elastic, ideally plastic soil models, while adequate for the determination of collapse of an embankment, is not appropriate for the prediction of critical state displacement behavior of a slope, (Zienkiewicz et al. 1978, Mizuno and Chen 1984, Zienkiewicz et al. 1985). The use of advanced plasticity models which satisfy the requirements of continuity and uniqueness of solution and have the capability of simulating a wide range of real effects in soils is essential for this type of analysis. A comprehensive review of the of the application of advanced plasticity models to the assessment of slope stability has been presented by Chen 1980.

The use of cap type, strain hardening plasticity models, (DiMaggio and Sandler 1971, Sandler 1976 and Sandler et al. 1976), provides a framework for the constitutive modeling of soils. Cap models are based on the classical incremental plasticity theory and are capable of representing the mechanical behavior of soils and rocks while satisfying all theoretical requirements for properly posed initial/boundary value dynamic problems. In other words, proper use of such models insures existence and uniqueness of solution as well as continuous dependence on the initial and boundary data. The cap model has a non-softening, convex yield surface as shown in Figure 1. For stress points within the yield surface, the material behaves elastically. For a stress point on the yield surface, the plastic strain rate vector is outwardly directed and normal to the yield surface in stress space. The characteristics of the cap model are illustrated in Figure 1. Cap models are able to permit inelastic hardening in hydrostatic loading, limit the amount of dilatancy during shear failure, and can provide a good fit to material property data. Cap models have been used extensively and successfully in ground shock analysis, (Sandler 1976 and Nelson and Baladi 1977), and to a limited extent, in the earthquake analysis of structures, (Vaughan et al. 1979, Mizuno and Chen 1984 and Daddazio, Ettouney and Sandler 1987).

Satisfactory seismic slope stability analyses require the prediction of critical state displacement behavior of an embankment. In the solution of a real problem with complicated geometry and fully nonlinear material behavior, the use of material models which lead to improperly posed initial/boundary value problems will result in totally unpredictable and

unreliable results. The cap model therefore provides a valid starting point, from both a theoretical and practical point of view, for the development of a specialized material model to be utilized in the analysis and design of embankments subjected to earthquakes.

Fitting a cap model to describe a given soil behavior generally requires that a suite of laboratory and field data (including cyclic uniaxial strain, triaxial compression and simple shear tests) be available for the material in question. Due to the fact that in practical cases, such test data may not be complete and/or the in situ conditions not sufficiently described, the cap model has sometimes been viewed "... as a sophisticated research oriented model that the consulting engineer may not find useful for everyday use." (Chen 1980).

The principal focus of our Phase I research was the development of a simplified cap model, specialized for use in seismic slope stability analyses. This new model embodies the theoretical integrity inherent in advanced plasticity formulations while at the same time being easy to use by a broad community of geotechnical engineers. In order to achieve this goal the following the specific tasks were undertaken:

1. the incorporation of a viscoelastic stress-strain relation into the cap model to simulate the effects of low amplitude cyclic hysteresis below the yield surface. This allows for a controlled amount of energy dissipation in cyclic loading and can be tuned to provide the correct damping at the shaking frequencies associated with typical earthquakes.
2. the incorporation of simplifying assumptions for the representation of the failure envelope, hardening rule and shape of the cap in order to reduce the number of parameters necessary to fit the model. The model can now be fit to soil properties obtained from data which is typically available to geotechnical engineers while maintaining the capability of the model to accurately simulate the inelastic behavior of soils. In addition, these simplifying assumptions improve the computational efficiency in the numerical implementation of the model.

Constitutive Model

The material model utilized in this study is an adaptation of the cap model described in Sandler and Rubin 1979. The model is extended to include viscoelasticity within the yield surface in order to model cyclic hysteresis at small to moderate shear strains as in Isenberg et al. 1978 and Sandler and Baron 1979. It was further simplified, as described below, to produce a version suitable for PC based slope stability analysis.

The viscoelastic portion of the model is described by

$$\dot{s} + \omega s = 2G_f \dot{e}^E + 2\omega G_s e^E \tag{1}$$

where s and e^E are the stress and viscoelastic strain deviators, ω is a relaxation rate and G_f, G_s represent the shear moduli under fast and slow loading, respectively, Figure 2. The volumetric behavior is elastic

$$J_1 = 3K\epsilon_v^E \tag{2}$$

where J_1 and ϵ_v^E are the traces of the stress and strain tensors and K is the bulk modulus.

As in the version of the cap model in Daddazio, Ettouney and Sandler 1987, the failure envelope is assumed to be the Drucker-Prager condition (Drucker and Prager 1952)

$$\sqrt{J_2'} = k - \alpha J_1 \tag{3}$$

where J_2' is the second invariant of the deviatoric stress and k and α are parameters related to the cohesion and angle of friction of the material.

In the current model, Figure 3, the cap, (which is usually elliptical as in Sandler and Rubin 1979, for example), is simplified to have a fixed center (at $J_1 = C_c$)

$$(C_c - J_1)^2 + R^2 J_2' = (C_c - X)^2 \tag{4}$$

where R is the cap shape factor. The cap size is proportional to $(C_c - X)$, where the variable X is governed by the hardening rule

$$X = \frac{\epsilon_v^P}{[D(W + \epsilon_v^P)]} \tag{5}$$

in which ϵ_v^P is the plastic volumetric strain, W is the maximum compaction and D is related to the rate of compaction at low pressure.

The cap simplifications introduced into the current model were designed to produce an efficiently running constitutive algorithm for the PC without sacrificing the ability of the model to characterize soil behavior. Thus, the value of R is fixed at $R = 3\sqrt{K/G_f}$ which, while generally consistent with the typical values of R for soils, enables a non-iterative algorithm to be written to compute the stress-strain behavior. The desirability of this choice for R will become clearer in the remainder of this section, which is devoted to a discussion of the constitutive algorithm.

The algorithm begins by computing a viscoelastic "trial value" for the stresses, i.e., a value based on the assumption that no failure or cap plasticity occurs. If the assumption is found to be false the stresses are revised by means of a "plastic correction" as described below. For reasons of accuracy under arbitrary loading paths, the viscoelastic trial values are obtained for a strain increment $\Delta\epsilon$ during a time step Δt as the exact solution for linear straining during the step $t_n \leq t \leq t_n + \Delta t$,

$$e^E(t) \approx e^{E_n} + \Delta e^E \left(\frac{t - t^n}{\Delta t}\right) \tag{6}$$

where e^{E_n} is the viscoelastic deviatoric strain at t_n.

Substituting equation 6 into equation 1 produces

$$\dot{s} + \omega s = 2G_f \frac{\Delta e^E}{\Delta t} + 2\omega G_s [e^{E_n} + \frac{\Delta e^E}{\Delta t}(t - t^n)] \tag{7}$$

which may be solved, using $s(t_n) = s^n$, to give

$$s(t) = s^n + 2G_s\frac{\Delta e^E}{\Delta t}(t - t^n) - \left[s^n - 2G_s e^{E_n} - 2\frac{G_f - G_s}{\omega}\frac{\Delta e^E}{\Delta t}\right]\left[1 - e^{-\omega(t-t_n)}\right] \quad (8)$$

at $t = t_n + \Delta t$:

$$s^{n+1} = s^n e^{-\omega\Delta t} + 2G_s e^{E_n}(1 - e^{-\omega\Delta t}) + 2[G_s + \frac{G_f - G_s}{\omega\Delta t}(1 - e^{-\omega\Delta t})]\Delta e^E \quad (9)$$

which is the viscoelastic trial deviatoric stress.

The viscoelastic trial stresses are then checked against the failure envelope and cap. If either or both of these surfaces is exceeded, the stress point is "corrected" so as to satisfy the appropriate yield condition and normal flow rule. For this purpose the "closest point projection" procedure described in Simo et al. 1988, is used in a fairly standard way. One case of particular interest is the cap itself. The flow rule is

$$\dot{\epsilon}^P_{ij} = \lambda\frac{\partial f}{\partial \sigma_{ij}} = -2(C_c - J_1)\lambda\delta_{ij} + R^2\lambda s_{ij} \quad (10)$$

or

$$\Delta\epsilon^P_v = -6\lambda(C_c - J_1) = \frac{(J_1^T - J_1)}{3K} \quad (11)$$

$$\Delta e^P_{ij} = R^2\lambda s_{ij} = \frac{1}{2G_f}\frac{(\sqrt{J_2'^T} - \sqrt{J_2'})s^T_{ij}}{\sqrt{J_2'^T}} \quad (12)$$

where the superscript T denotes a viscoelastic trial value. Equations 11 and 12 imply

$$C_c - J_1 = \frac{C_c - J_1^T}{1 + 18K\lambda} \quad (13)$$

$$\sqrt{J_2'} = \frac{\sqrt{J_2'^T}}{1 + 2G_f R^2\lambda} \quad (14)$$

so that, if we choose

$$18K = 2G_f R^2 \quad (15)$$

the correction from the "T" values will be radial toward the point $(J_1 = C_c, s_{ij} = 0)$ in stress space. If $\mu = \frac{1}{(1+18K\lambda)}$ equations 13 and 14 become

$$C_c - J_1 = \mu(C_c - J_1^T) \quad (16)$$

$$\sqrt{J_2'} = \mu\sqrt{J_2'^T} \quad (17)$$

and the cap equation 4 may be written as

$$\mu\sqrt{(C_c - J_1^T)^2 + R^2 J_2'^T} = C_c - X \tag{18}$$

Equations 5,16,17 and 18 together with the volumetric plastic "correction" given by

$$J_1 = J_1^T - 3K(\epsilon_v^P - \epsilon_v^{P_o}) \tag{19}$$

where $\epsilon_v^P = \epsilon_v^{P_o}$ at $t = t_n$, form a system of equations which can be solved for μ,J_1, $\sqrt{J_2'}$,X and ϵ_v^P. Appendix I contains the FORTRAN implementation of the algorithm described in this section.

Fitting the Proposed Model

One of the primary goals of this research was to formulate the new model in terms of the data that is typically available to geotechnical engineers. The input parameters that the engineer must provide in order to use the model along with representative values for a broad grouping of soils are given as follows:

1. the bulk modulus, K. Typical values for soils are several thousands of psi (several tens of thousands kPa).

2. a "fast" and "slow" shear modulus, G_f and G_s, respectively. Typical values for G_s are half the bulk modulus. A value of $1.0G_s < G_f \leq 1.5G_s$ is typical for a large range of soils. These parameters are related to the size of the elliptical hysteresis loop and hence the amount of energy dissipated through viscous damping in the material.

3. a viscoelastic relaxation parameter, ω. This parameter is related to the frequency of vibration of the system. For seismic events, values are typically several sec^{-1} .

4. the cohesion, c, and angle of internal friction ϕ, of the soil. Typical values for these parameters are tens of psi (hundreds of kPa) and tens of degrees. These two parameters are used to determine the failure envelope by relating the Drucker-Prager criterion of equation 3 to the Coulomb criterion in three dimensional principal stress space.

5. the maximum compactibility of the soil, W. A value of on the order of one tenth is typical. Note that $W > 0$.

6. the ratio of the loading to unloading bulk modulus at low pressure, D. Typical values for this parameter are on the order of one tenth. Note that $0. < D < 1.0$.

It is extremely important to note that the values indicated in items one through six above are to be used as guidelines. The values, though typical for a wide range of soils, none the less must be verified before they are used in any analysis.

Case Study

In an effort to exercise the new cap model, the formulation described in the previous section was implemented in the finite element program SADNESS (Seismic Analysis for Dynamic Nonlinear Earth Slope Stability). The details of this program are elaborated in Daddazio, Ettouney and Sandler 1987. This program employs a constant strain triangular finite element together with an explicit nonlinear dynamic updated Lagrangian kinematic formulation and a cap type soil constitutive relation to simulate the progressive failure analysis of embankments subjected to seismic loading. Both material and geometric nonlinearities are present in the analysis.

The case study makes use of the vertical slope configuration described in Mizuno and Chen 1984, shown in Figure 4, subjected to the earthquake acceleration time history shown in Figure 5. The ground condition in the absence of the slope and the material properties of the embankment assumed by Mizuno and Chen are indicated in Figure 6.

The in situ state of stress and deformation in the slope prior to the application of the seismic excitation must be determined. This is accomplished by gradually increasing the self weight of the soil via a time varying ramp function. The slope of the ramp function is chosen such that inertia forces resulting from the application of the soil self weight are negligible.

The deformed geometry for the initial condition of the embankment is shown in Figure 7. Ground settlement of the top surface is 1.33m (4.36ft). The maximum horizontal displacement occurs at point B in Figure 7. The value of this displacement is 0.18m (7.25 in). It is expected that at the onset of sliding, this point would be the intersection of the slip surface with the vertical face of the embankment. Comparing this initial state using the new model with the results of Daddazio, Ettouney and Sandler 1987 which utilized the cap model of Sandler and Rubin 1979, indicates a similar response at this load level. It should be mentioned at this point that conventional methods indicate that this slope is close to the limit of **static** stability, an effect confirmed by the dynamic analysis performed here. The seismic loading presented in Figure 5 is applied as a horizontal base motion to the finite element mesh of Figure 4.

The results of Daddazio, Ettouney and Sandler 1987 are summarized here as a basis for comparison with the same analysis conducted with the new cap model. The horizontal velocity and displacement time histories of point **B** relative to point **A**,(as indicated in Figure 7) are shown in Figure 8. These indicate that failure of the slope commences at approximately 5.25 sec. The progressive failure of the embankment is indicated by the sequence of "snapshots" comprising Figure 9. This figure displays the deformed configuration of the slope relative to the initial configuration of Figure 7. Also indicated in Figure 9 is the relative velocity field of the embankment. The relative velocity vectors are defined as the difference between the velocity at a nodal point and that of the toe (point A in Figure 9a).

The slope was re-analyzed using the new cap model. The properties used to fit the new model are as follows:

$$
\begin{aligned}
K &= 2.892 \text{ ksi } (19.94 \times 10^3 \text{ kPa}) \\
G_f &= 1.34 \text{ ksi } (9.2 \times 10^3 \text{ kPa}) \\
G_s &= 1.34 \text{ ksi } (9.2 \times 10^3 \text{ kPa}) \\
c &= 661 \text{ psf } (31.6 \text{ kPa}) \\
\phi &= 8.18^\circ \\
\omega &= 5\,\text{sec}^{-1} \\
W &= 0.06 \\
D &= 0.1
\end{aligned}
$$

It should be noted that in the absence of material test data, the parameters of this model are not directly equivalent to the parameters of the CAP75 model of Sandler and Rubin 1979. As such, approximations were made in some of the values listed above. The value of the cohesion, c, and angle of friction, ϕ, were adjusted from those shown in Figure 6 so that the failure envelope in each analysis is equivalent. The values of G_f and G_s were chosen to be the same in order to eliminate any viscoelastic behavior in this initial analysis. Hence the new model will behave **elastically** below the yield surface. The ratio of the loading to unloading bulk modulus, D, was chosen such that the hardening behavior of the new model, given by equation 5, simulated, as closely as possible, the hardening behavior of the CAP75 model. In the initial comparison between the new model and CAP75, the value of ω is not meaningful due to the fact that viscoelastic effects are not being considered since $G_f = G_s$.

The results of this comparison are shown in Figure 10. The horizontal component of displacement of point **B** relative to point **A** (as indicated in Figure 9a) is displayed in Figure 10. It is readily apparent that both models indicate failure of the embankment due to the given seismic excitation. In both models, the failure commences at 5.25 seconds. The sliding is more "rapid" with CAP75 but this can be attributed to differences in the two models in the shape of the cap, hardening response and tension behavior.

Two additional runs were made to determine the effect of viscous damping in the soil, as simulated by the viscoelastic part of the new model. In the absence of test data, the values of G_f and G_s were chosen to bracket the given value of shear modulus indicated in Figure 6. The two sets of values used were:

$G_f = 1.37$ ksi and $G_s = 1.31$ ksi
$G_f = 1.45$ ksi and $G_s = 1.23$ ksi

Each set of values corresponds to a different amount of material damping. The results of these two runs are shown in Figure 11 together with the previous case ($G_f = G_s =$ 1.34 ksi), which is undamped. The displacement in this figure corresponds to the horizontal component of displacement of point **B** relative to point **A** as indicated in Figure 9a.

In these analyses the seismic excitation has a duration of 20 sec as shown in Figure 5. The effect of the viscoelastic part of the new cap model on the deformation of the embankment is clearly indicated. It is apparent that for the case of no viscous damping and the damping associated with case 1, the embankment has failed. For the viscous damping associated with case 2 , the sliding soil mass comes to rest with a permanent horizontal deformation of 12 in (0.3048 m). The value of viscous damping to be used of course depends on material test data. For design purposes, in order to be conservative, a low value of viscous damping is appropriate.

Conclusions

The broad goal of our Phase I research was the development of a simplified cap model specialized for seismic analysis of embankments. The specific objectives to be met were the following:

1. to incorporate a viscoelastic stress-strain relation into the cap model to simulate the effects of low amplitude cyclic hysteresis below the yield surface,

    - The results of the analyses presented in this report indicate that this new cap model can simulate the energy dissipation in soils during cyclic loading, (Figure 11). This change was effected through the addition of a standard solid model in order to represent the viscoelastic behavior of the material within the yield surface.

2. to incorporate simplifying assumptions in the type of failure envelope, hardening rule and shape of the cap in order to reduce the number of parameters necessary to fit the model to those properties which can be obtained from the data which is most typically available to the geotechnical engineer,

    - The results of the analyses presented herein indicate that the new model, although simplified, can adequately represent the progressive failure of an embankment when compared to a cap model fit to materials for which a full complement of test data exists (Figure 10).

    - The parameters necessary to fit the new model have been recast in such a way that they are directly related to data ordinarily accessible to geotechnical engineers.

    - As the long range goal of this research is the development of a PC based computer program capable of simulating the progressive failure of slopes subjected to seismic shaking, computational efficiency of the constitutive model is of paramount importance. Preliminary benchmarks indicate that calculations made with this new model are approximately twice as fast as those made with a standard cap model such as CAP75 described in Sandler and Rubin 1979.

The potential for damage to lifeline systems and transportation networks not to mention loss of life from earthquake induced slope failure is quite large. There is a broad base of world wide interest in improving the understanding of this phenomenon in order to mitigate the damage from it.

The result of this Phase I research has been the development of a theoretically sound, qualitatively effective and computationally efficient soil model to be used in practical progressive failure analysis and design of embankments subjected to earthquakes. The successful completion of this research establishes the foundation for the incorporation of this new model into a PC based dynamic nonlinear finite element computer program which would bring the capability of rational seismic slope stability analysis and design to a broad spectrum of engineers. The results of a typical analysis would include the location of the failure surface within the slope and its variation with time, permanent deformations of the embankment and the assessment of the effectiveness of design countermeasures to prevent or limit sliding. Parametric studies could be implemented to ascertain the effects of earthquake intensity and frequency content as well as slope geometry on stability. In addition, such a program could be utilized by researchers in order to enhance the understanding of existing analysis methods and to suggest modifications or improvements to them.

Acknowledgment

The writers would like to thank Mohammed Ettouney and David Rubin for their gracious assistance during the course of this research.

References

Chen, W., "Plasticity in Soil Mechanics and Landslides," *Journal of the Engineering Mechanics Division*, ASCE, Vol. 106, No. EM3, Proc. Paper 15460, pp. 443-464, (1980).

Chen, W.F., Chang, C.J. and Yao, J., "Limit Analysis of Earthquake-Induced Slope Failure," *Proceedings*, 15th Annual Meeting of the Society of Engineering Science, R.L. Sierakowski, ed., University of Florida, Gainsville, FL, pp. 533-538, (1978).

Chugh, A.K., "Slope Stability Analysis for Earthquakes," *International Journal for Numerical and Analytical Methods in Geomechanics*, Vol. 6, pp. 307-322, (1982).

Daddazio, R.P., Ettouney, M.M. and Sandler, I.S., "Nonlinear Dynamic Slope Stability Analysis," *Journal of Geotechnical Engineering*, ASCE, Vol. 113, No. 4, pp. 285-298, (1987).

DiMaggio, F.L. and Sandler, I.S., "Material Model for Granular Soils," *Journal of the Engineering Mechanics Division*, ASCE, Vol. 97, No. EM3, pp. 935-949, (1971).

Drucker, D.C., and Prager, W., "Soil Mechanics and Plastic Analysis or Limit Design," *Quarterly of Applied Mathematics*, Vol. 10, No. 2, pp. 157-175, (1952).

Isenberg, J., Vaughan, D.K., and Sandler, I.S., "Nonlinear Soil-Structure Interaction," *Report No. EP-NP-945*, Final Report to EPRI, Weidlinger Associates, Palo Alto, CA, (1978).

Mizuno, E., and Chen, W.F., "Plasticity Models for Seismic Analysis of Slopes," *Soil Dynamics and Earthquake Engineering*, Vol. 3, No. 1, pp 2-7, (1984).

Nelson, I., and Baladi, G.Y., "Outrunning Ground Shock Computed with Different Models," *Journal of the Engineering Mechanics Division*, ASCE, Vol. 103, No. EM3, pp. 377-393, (1977).

Newmark, N.M., "Effects of Earthquakes on Dams and Embankments," *Geotechnique*, London, England, Vol. 15, No. 2, pp. 139-160, (1965).

Sandler, I.S., "The Cap Model for Static and Dynamic Problems," *Site Characterization - U.S. Symposium on Rock Mechanics*, W.S. Brown, ed., University of Utah, Salt Lake City, Utah, pp. 1A2-1-1A2-11, (1976).

Sandler, I.S., DiMaggio, F.L., and Baladi, G.Y., "Generalized Cap Model for Geological Materials," *Journal of the Geotechnical Engineering Division*, ASCE, Vol. 102, No. GT7, pp. 683-399, (1976).

Sandler, I.S. and Baron, M.L., "Recent Developments in the Constitutive Modeling of Geological Materials," *Proceedings*, Third International Conference on Numerical Methods in Geomechanics, W. Wittke, ed., Balkema, Rotterdam, Netherlands, pp. 363-376, (1979).

Sandler, I.S. and Rubin, D., "An Algorithm and a Modular Subroutine for the Cap Model," *International Journal for Numerical and Analytical Methods in Geomechanics*, Vol. 3, pp. 173-186, (1979).

Sandler, I.S., DiMaggio, F.L., and Baron, M.L., "Extension of the Cap Model - Inclusion of Pore Pressure Effects and Kinematic Hardening to Represent an Anisotropic Wet Clay," *Mechanics of Engineering Materials*, C. Desai and R. Gallagher, eds., John Wiley & Sons, New York, pp.547-578, (1984).

Seed, H.B., "A Method for Earthquake Resistant Design of Earth Dams," *Journal of the Soil Mechanics and Foundations Division*, ASCE, Vol. 92, No. SM1, pp. 13-41, (1966).

Seed, H.B., and Martin, G.R., "The Seismic Coefficient in Earth Dam Design," *Journal of the Soil Mechanics and Foundations Division*, ASCE, Vol. 92, No. SM3, pp. 25-58, (1966).

Seed, H. B., "Earth Slope Stability During Earthquakes," *Earthquake Engineering*, R.L. Wiegel, ed., Prentice-Hall, Inc., Englewood Cliffs, NJ, pp. 383-390, (1970).

Simo, J.C., Wu, J., Pister, K.S. and Taylor, R.L., "Assessment of Cap Model: Consistent Return Algorithms and Rate-Dependent Extension," *Journal of Engineering Mechanics Division*, ASCE, Vol. 114, pp. 191-218, (1988).

Vaughan, D., et al., "Preliminary Data Report of a Pretest Analysis of Soil-Structure Interaction and Structural Response in Low-Amplitude Explosive Testing of the Heissdampfreaktor," *Report Number R7943*, Weidlinger Associates, Palo Alto, CA, (1979).

Zienkiewicz, O.C., Chang, C.T., and Hinton, E., "Nonlinear Seismic Response and Liquefaction," *International Journal for Numerical and Analytical Methods in Geomechanics*, Vol.2, pp. 381-404, (1978).

Zienkiewicz, O.C., Leung, K.H. and Pastor, M., "Simple Model for Transient Soil Loading in Earthquake Analysis. I. Basic Model and its Application," *International Journal for Numerical and Analytical Methods in Geomechanics*, Vol. 9, pp. 453-476, (1985).

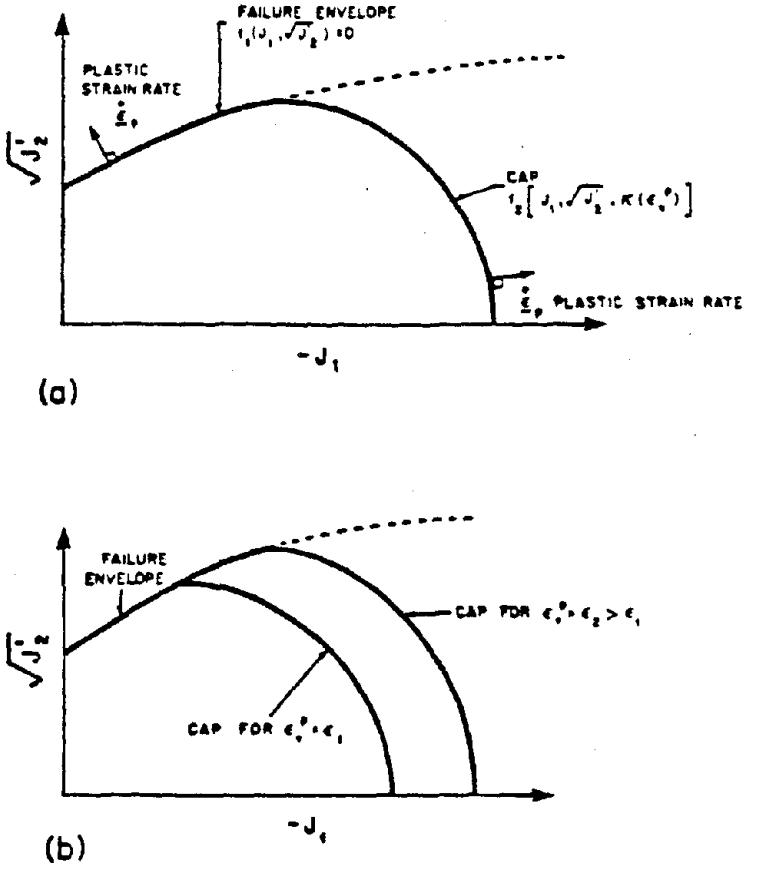

FIG. 1.- CAP MODEL

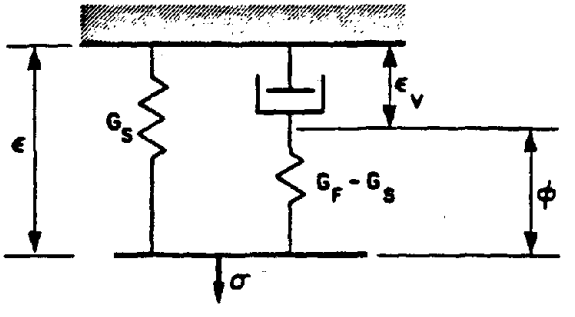

FIG. 2.- VISCOELASTIC MODEL

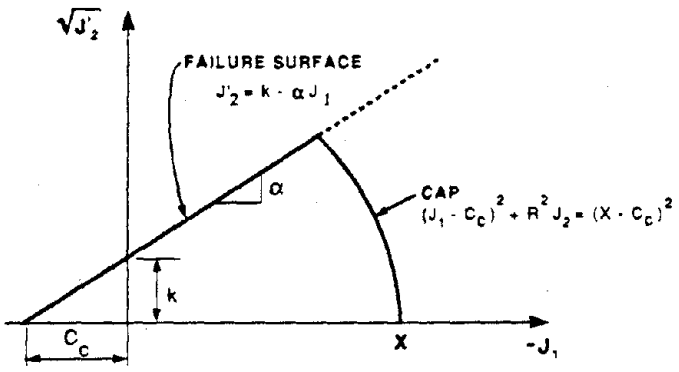

FIG. 3. - Proposed Cap Model for Seismic Analysis

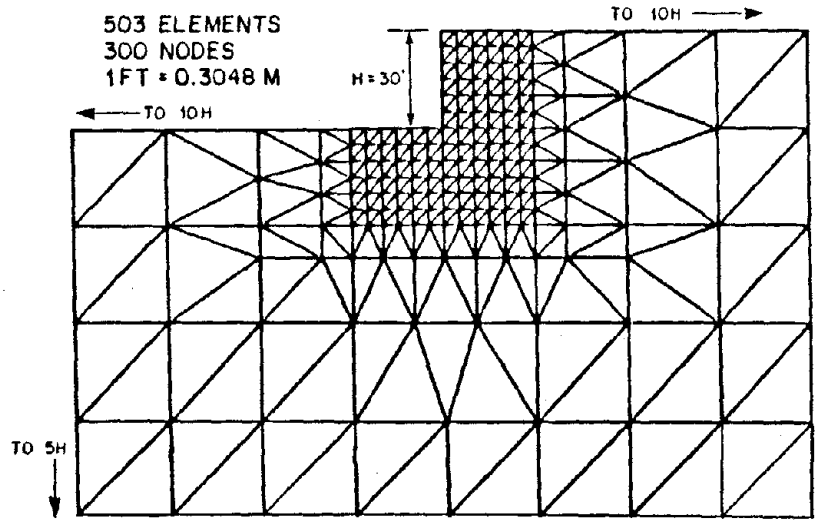

FIG. 4. - Finite Element Discretization for Case Study

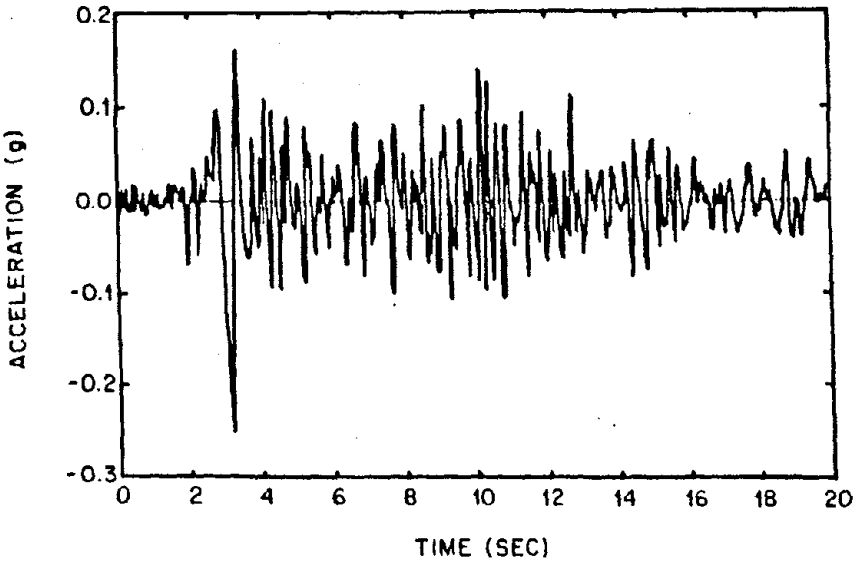

FIG. 5. - Earthquake Acceleration Time History

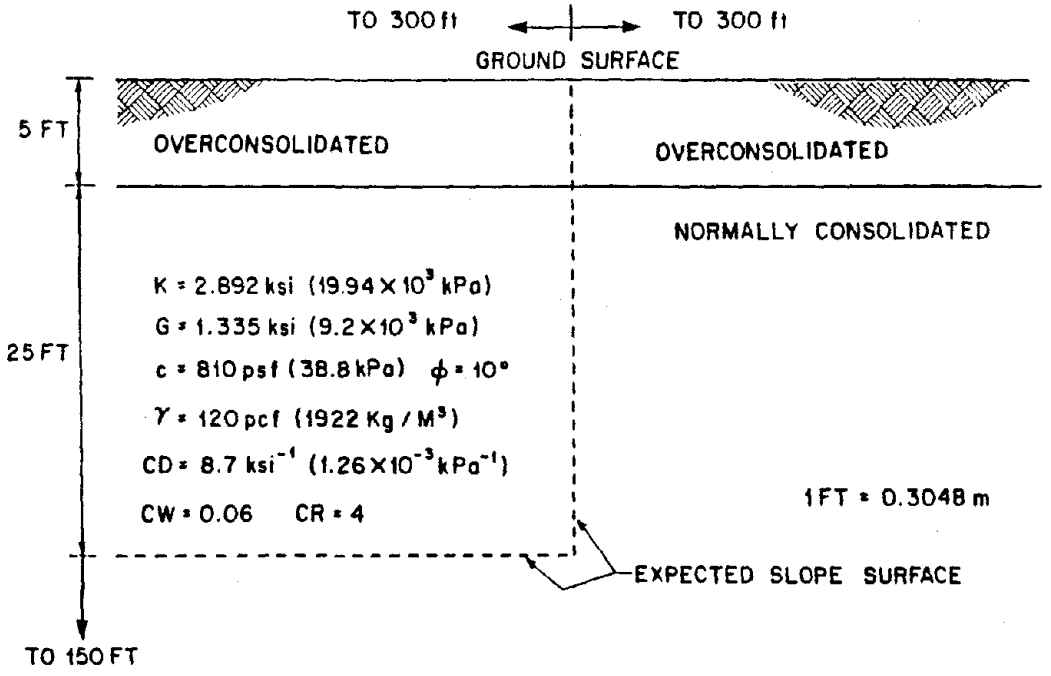

FIG. 6. - Ground Condition for Case Study

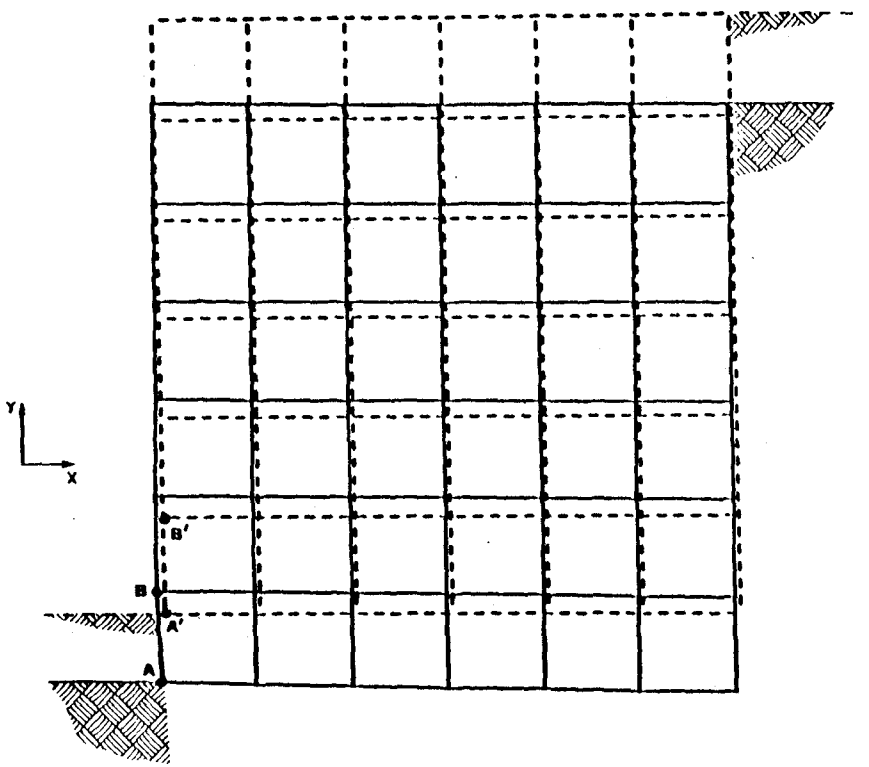

FIG. 7. - Slope Deformation Due to Self Weight

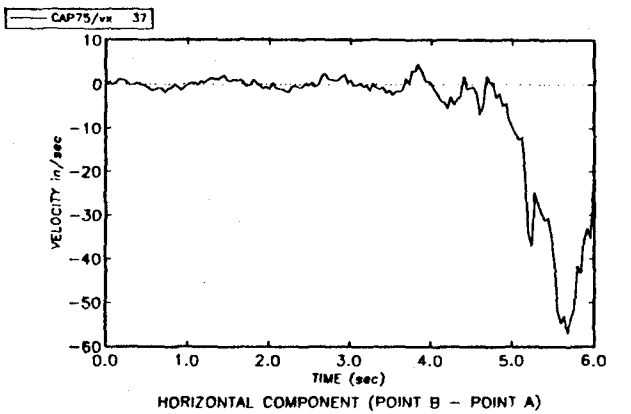

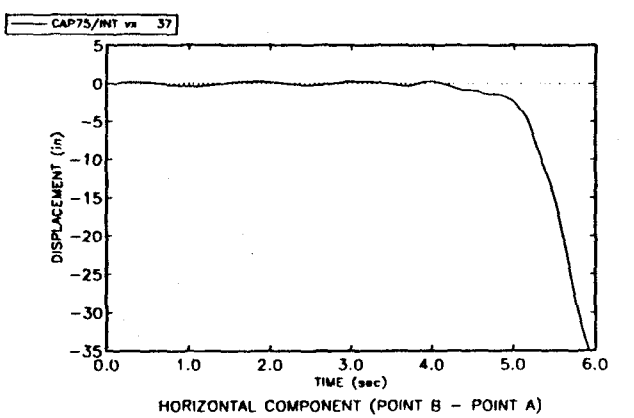

FIG. 8. - Horizontal Component of Velocity and Displacement

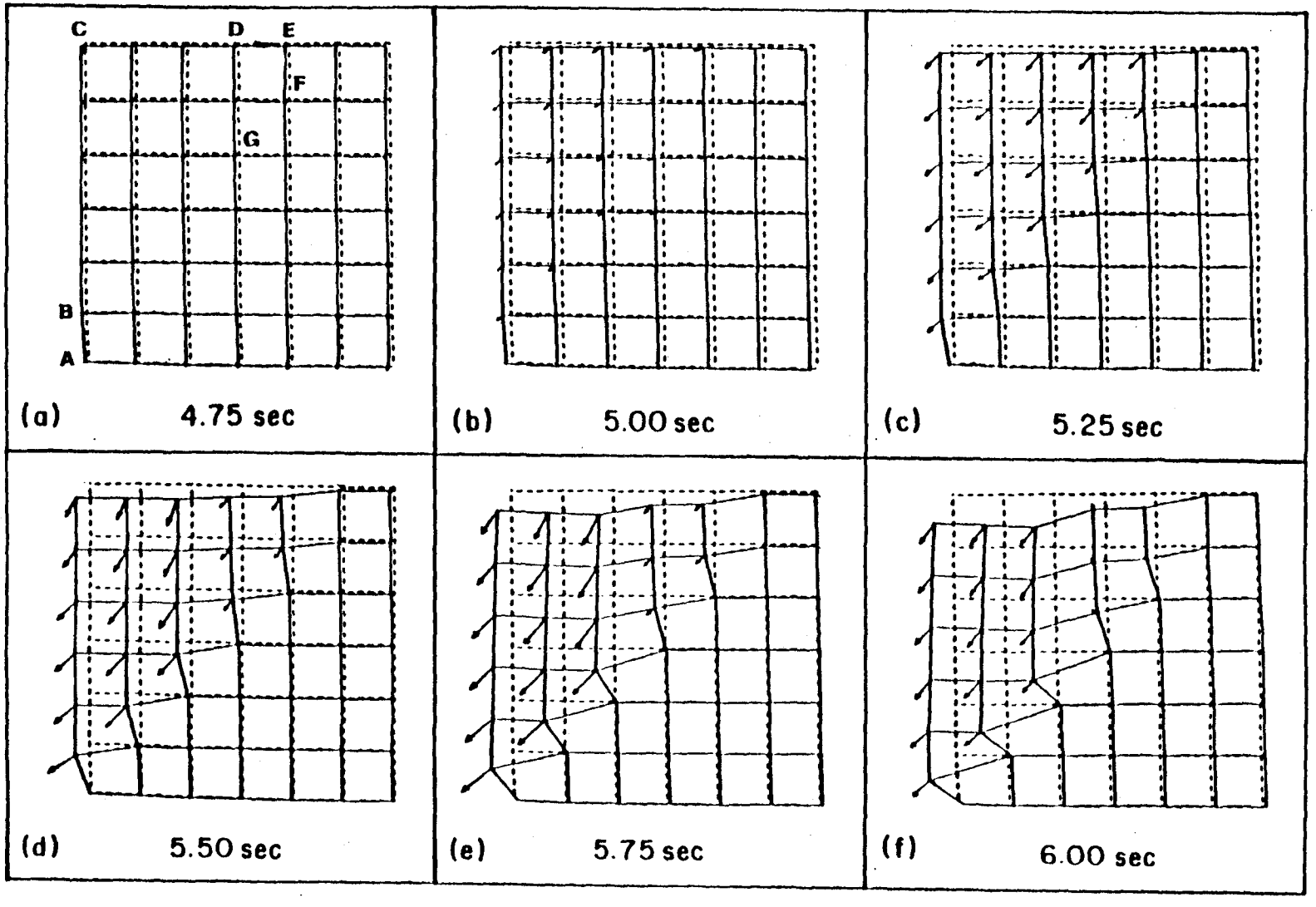

FIG. 9. - Progressive Failure of Embankment

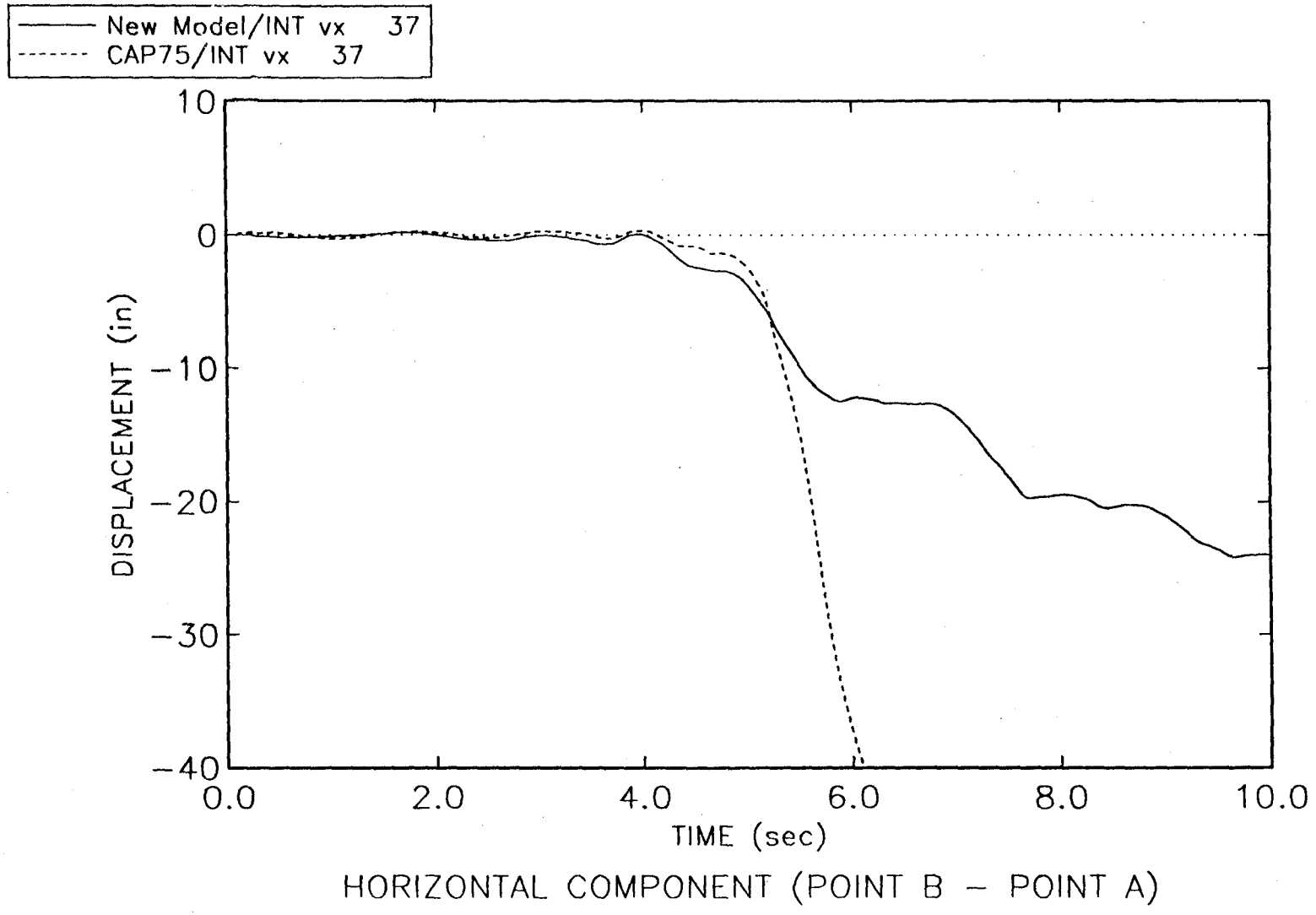

FIG. 10. - Comparison of Proposed Model and CAP75

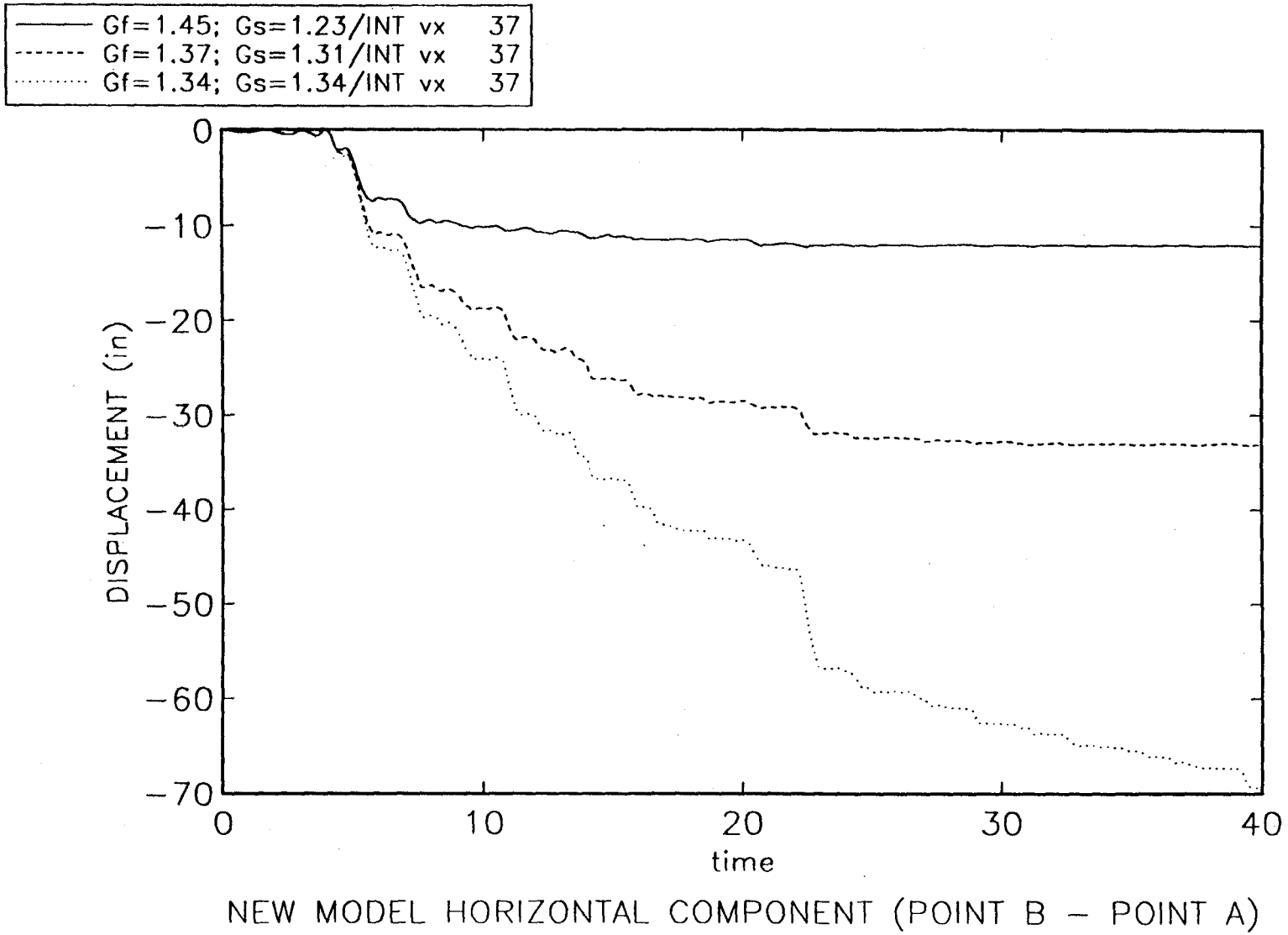

FIG. 11. - Displacement Time Histories Varying Viscous Damping

Appendix I

The algorithm described in this report forms the basis for the subroutine **SADCAP**. A compiled listing of this routine is presented in this Appendix. The routine is set up for two dimensional computations. The comments in the listing of the subroutine describe the the required calling arguments.

In order to use **SADCAP**, an auxiliary preprocessor, subroutine **INITSD**, is convenient. This routine computes the values of the variables in labelled commom /SPROP/ from the user input values stored in labeled common /PROP/. The variables in /PROP/ are self explanatory . The variable *ktype* takes the value one for soil and two for rock. The variables in the argument list for routine **INITSD** are *dt* which is the integration time step, and *xint* which is the initial intersection of the cap with the J_1 axis.

```
      subroutine sadcap(sj1,s,e,depsv,de,x,mtype)
c...
c... two-dimensional simplified cap model
c... sj1,depsv = -3*pressure, increment of volume strain
c... s,e,de = array of deviatoric components of stress,
c...        viscoelastic strain, and increment of strain
c...
      dimension s(3),e(3),de(3)
      common /sprop/ ltype,threek,hold,tgsrel,tshear,fa,fk,
     1       cc,cd,cr,cw,rho,fakv,sopar2,ccb,cd3,cd3k,
     2         c4c,cwd
c... viscoelastic trial
      mtype=1
      sj1=sj1+threek*depsv
      do 100 i=1,3
        s(i)=hold*s(i)+tgsrel*e(i)+tshear*de(i)
  100 continue
      ratio=1.
      sj2=sqrt(s(1)*s(1)+s(2)*s(2)+s(1)*s(2)+s(3)*s(3))
      fft=sj2-fa*(cc-sj1)
      if(fft.le.0.) goto 700
c... failure
      sj1f=sj1-fft/fakv
      if(sj1f.ge.cc) goto 200
c... check for cap location
      sj1cap=cc-(cc-x)/sopar2
      if(sj1.lt.sj1cap) goto 500
      mtype=2
      if(sj1f.gt.sj1cap) goto 300
c... corner dilatancy
      mtype=23
      sj1=sj1cap
      goto 600
c... dilatancy effect on cap
c...  tension
  200 continue
        mtype=0
        sj1=cc
        ratio=0.
  300 continue
        if(ltype.ne.1) goto 400
        evp=cwd*x/(1.-cd*x)+(sj1-sj1f)/threek
        x=min(sj1f,evp/(cd*(cw+evp)))
  400 continue
        if(mtype.eq.0) goto 800
        sj1=sj1f
        goto 600
c... corner compaction
  500 continue
        b=ccb-sj1/threek-cwd*x/(1.-cd*x)
        evp=0.5*(sqrt(b*b+c4c)-b)-cw
        x=evp/(cd*(cw+evp))
        sj1=cc-(cc-x)/sopar2
        mtype=32
```

```
 600  continue
          ratio=fa*(cc-sj1)/sj2
          goto 800
 700  continue
          fct2=(cc-sj1)*(cc-sj1)+(cr*sj2)*(cr*sj2)
          if(fct2.le.(cc-x)*(cc-x)) goto 800
c... cap
          mtype=3
          ft=sqrt(fct2)
          evpo=cwd*x/(1.-cd*x)
          b=(cc-sj1)*(1.+cd*(ft-cc))/(cd3k*ft)-evpo-cw
          c4=4.*(cc-sj1)*cw/(cd3k*ft)
          evp=0.5*(sqrt(b*b+c4)-b)-cw
          x=evp/(cd*(cw+evp))
          dsj1=threek*(evpo-evp)
          ratio=1.-dsj1/(cc-sj1)
          sj1=sj1+dsj1
c... calculate stresses and viscoelastic strain
 800  continue
          do 900 i=1,3
             e(i)=e(i)+de(i)-(1.-ratio)*s(i)/tshear
             s(i)=ratio*s(i)
 900   continue
       return
       end
```

```
      subroutine initsd(dt,xint)
      common/prop/ktype,bulk,gf,gs,omega,c,phi,ddk,w
      common /sprop/ ltype,threek,hold,tgsrel,tshear,fa,fk,
     1       cc,cd,cr,cw,rho,fakv,sopar2,ccb,cd3,cd3k,
     2         c4c,cwd
c.... sprop parameters
      ltype=ktype
      cw=w
      aphi=phi*3.14/180.
      threek=3.0*bulk
      hold=exp(-omega*dt)
      omhold=1.0-hold
      if(hold.ge..9999) omhold=omega*dt
      tgsrel=2.0*gs*omhold
      tshear=2.0*(gs+(gf-gs)*omhold/(omega*dt))
      fa=2.0*sin(aphi)/(sqrt(3.0)*(3.0-sin(aphi)))
      fk=6.0*c*cos(aphi)/(sqrt(3.0)*(3.0-sin(aphi)))
      cc=fk/fa
      fakv=threek*fa/(threek*fa**2+tshear/6.0)
      cr=sqrt(6.0*threek/tshear)
      sopar2=sqrt(1.0+(fa*cr)**2)
      cd=(1.0-ddk)/(3.0*ddk*bulk*cw)
      ccb=((1.0/cd-cc)/sopar2+cc)/threek-cw
      cd3k=cd*threek
      c4c=4.0*cw/(cd3k*sopar2)
      cwd=cw*cd
c.... check initial value of x
      xint=min(xint,cc)
      return
      end
```